LOW-DIMENSIONAL AND DISORDERED SYSTEMS

Linear diatomic crystal: single-electron states and large-radius excitons

V. M. Adamyan and O. A. Smyrnov[a)]

Department of Theoretical Physics, Odessa I. I. Mechnikov National University, 2 Dvoryanskaya St., Odessa 65026, Ukraine

(Submitted November 13, 2008; revised January 4, 2009)
Fiz. Nizk. Temp. **35**, 503–509 (May 2009)

The large-radius exciton spectrum in a linear crystal with two atoms in the unit cell is obtained using the single-electron eigenfunctions and band structure found by the zero-range potentials method. The ground-state exciton binding energies for the linear crystal in vacuum turn out to be larger than the corresponding energy gaps for any set of the crystal parameters.
 [DOI: 10.1063/1.3132746]

I. INTRODUCTION

The study of the quasi-one-dimensional semiconductors with cylindrical symmetry became an urgent problem as soon as investigations of semiconducting nanotubes had been launched. One of the most important trends of research in this field is the study of the optical spectra of such systems, which should include the exciton contributions.[1–9] Evidently, the quasi-one-dimensional large-radius exciton problem can be reduced to a 1D system of two quasi-particles with a potential having a Coulomb attraction tail. Due to the parity of the interaction potential the exciton states should split into odd and even series. In Ref. 10 we show that for the bare and screened Coulomb interaction potentials the binding energy of even excitons in the ground state well exceeds the energy gap (in the same work we also discuss the factors which prevent the collapse of single-electron states in isolated semiconducting single-walled carbon nanotubes (SWCNTs). But the electron-hole (e-h) interaction potential and thus the corresponding exciton binding energies may depend noticeably on the electron and hole charge distributions. It is therefore worthwhile to ascertain whether the effect of seeming instability of single-electron states near the gap is inherent to the all quasi-one-dimensional semiconductors in vacuum or maybe takes place only in SWCNTs for the specific localization of electrons (holes) at their surface and weak screening by the bound electrons. That is why we consider here the simplest model of a quasi-one-dimensional semiconductor with cylindrical symmetry, namely the linear crystal with two atoms in the unit cell. The electrons (holes) in this crystal are simply localized at its axis.

The aim of this work is only a qualitative analysis of the effect mentioned. For study of electron structure of the 1D crystal concerned, we apply here the zero-range potentials (ZRP) method[11,12] (see Sec. II). The matter is that results on the band structure and single-electron states, obtained by this method for SWCNTs in Refs. 13 and 14, appeared to be in good accordance with the experimental data and results of *ab initio* calculations related to the band states. For specificity we use the linear crystal parameters (the electron bare mass, lattice parameters) taken from works on nanotubes.[13,14] In Sec. III we obtain the e-h bare interaction potential and that screened by the crystal band electrons, and then the large-radius exciton spectrum for the linear crystal in vacuum. All these data are used in Sec. IV, where we present results of calculations for crystals with different lattice periods (which also means different band structures).

As it turns out, the binding energy of even excitons in the ground state well exceeds (~2–5 times) the energy gap for the linear crystal in vacuum, and the screening by the crystal band electrons is negligible. Note that this result was obtained within the framework of exactly solvable ZRP model with feasible parameters. Therefore, the instability effect mentioned may take place not only for the considered simplest case but, most likely, also for other quasi-one-dimensional isolated semiconductors in vacuum.

II. SINGLE-ELECTRON BAND STRUCTURE AND EIGENFUNCTIONS OF BAND ELECTRONS

We have obtained the single-electron states in the linear crystal using the ZRP method.[11,12] The main point of this method is that the interaction of an electron with atoms or ions of a lattice is described, instead of by some periodic potential $V(\mathbf{r})$, by the sum of Fermi pseudo-potentials[11]

$$(1/\alpha)\sum_l \delta(\rho_l)(\partial/\partial\rho_l)\rho_l$$

($\rho_l=|\mathbf{r}-\mathbf{r}_l|$, $\mathbf{r}_l$ are the atom location points, α is a certain fitting parameter) or equivalently by the set of boundary conditions imposed on the single-electron wave function ψ at points $\mathbf{r}_l$:

$$\lim_{\rho_l\to 0}\left\{\frac{d}{d\rho_l}(\rho_l\psi)(\mathbf{r})+\alpha(\rho_l\psi)(\mathbf{r})\right\}=0.$$

Then the electron wave functions satisfy the Schrödinger equation for a free particle for $\mathbf{r}\neq\mathbf{r}_l$. Therefore we seek them for the linear crystal in the form:

$$\psi(\rho_n^A,\rho_n^B)=\sum_{n=-\infty}^{\infty}A_n\frac{\exp(-\kappa\rho_n^A)}{\rho_n^A}+\sum_{n=-\infty}^{\infty}B_n\frac{\exp(-\kappa\rho_n^B)}{\rho_n^B}, \quad (1)$$

where indices A and B denote the two monatomic sublattices of the diatomic lattice,

$$\rho_n^A = |\mathbf{r} - \mathbf{r}_n^A| \text{ and } \rho_n^B = |\mathbf{r} - \mathbf{r}_n^B|,$$

n enumerates all the sublattices points, $\kappa = \sqrt{2m_b|E|}/\hbar$, $E < 0$ is the electron energy, and m_b is the bare mass. For specificity, following Refs. 13 and 14, from now on we take $m_b \simeq 0.415 m_e$ and the ZRP parameter $\alpha = \sqrt{2m_b|E_{\text{ion}}|}/\hbar$, where E_{ion} is the ionization energy of an isolated carbon atom. According to Refs. 13 and 14, with these α and m_b the ZRP method reproduces single-electron spectra of such quasi-one-dimensional structures as SWCNTs within the accuracy of existing experiments. One can take infinite limits for the series in (1) even for the finite crystal, because the terms of these series decrease exponentially with increasing n.

According to the ZRP method the wave functions (1) at the all sublattices points should satisfy the following boundary conditions:

$$\lim_{\rho_l^i \to 0} \left\{ \frac{d}{d\rho_l^i} (\rho_l^i \psi)(\mathbf{r}) + \alpha (\rho_l^i \psi)(\mathbf{r}) \right\} = 0, \tag{2}$$

here $i = \{A, B\}$ according to each sublattice.

Further we suppose that the linear crystal lies along the z axis, and thus $\mathbf{r}_n^A = nd\mathbf{e}_z$ and $\mathbf{r}_n^B = (nd + a)\mathbf{e}_z$, where $\mathbf{e}_z$ is the z axis unit vector, a is the distance between atoms in the unit cell of the crystal, and $d > 2a$ is the distance between the neighbor atoms in each sublattice. Note that $d = 2a$ corresponds to the metallic monatomic crystal, and for the case $d < 2a$ the smallest distance between atoms in the crystal is $d - a < a$.

Substituting (1) into (2) and applying the Bloch theorem ($A_n = A \exp(iqdn)$, $B_n = B \exp(iqdn)$, q is the electron quasimomentum), we get two equations for the amplitudes A and B:

$$\begin{cases} AQ_1 + BQ_2 = 0, \\ AQ_2^* + BQ_1 = 0, \end{cases} \tag{3}$$

where

$$Q_1(\kappa, q) = \alpha - \frac{1}{d} \ln(2[\cosh \kappa d - \cos qd]), \tag{4}$$

$$Q_2(\kappa, q) = \sum_{n=-\infty}^{\infty} \frac{\exp(-\kappa|nd + a| + iqnd)}{|nd + a|}. \tag{5}$$

Setting $d = ja$:

$$Q_2(\kappa, q) = \frac{1}{a} \int_0^1 \left(\frac{\exp[-\kappa a]}{1 - x^j \exp[d(iq - \kappa)]} + \frac{x^{j-2} \exp[\kappa a]}{\exp[d(iq + \kappa)] - x^j} \right) dx \tag{6}$$

for each real $j > 2$.

From (3) we get two equations, which define the band structure of the crystal:

$$Q_1(\kappa_1, q) - |Q_2(\kappa_1, q)| = 0, \tag{7}$$

$$Q_1(\kappa_2, q) + |Q_2(\kappa_2, q)| = 0. \tag{8}$$

Equation (7) defines the conduction band and equation (8) defines the valence band (see Sec. IV, Fig. 1). So the electron and hole effective masses can be simply obtained from (7) and (8), respectively.

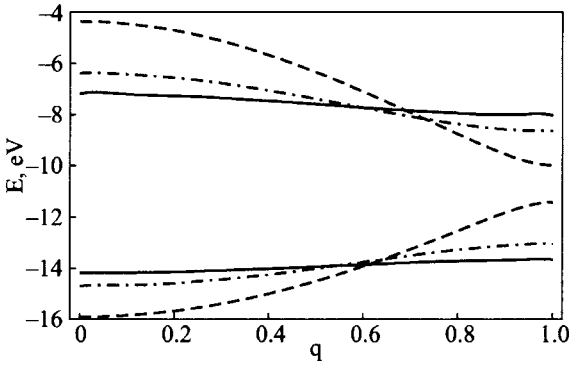

FIG. 1. The band structure of the linear crystal with parameters: $j = 2.1$ (dashed line), $j = 2.5$ (dot-and-dash line), and $j = 3$ (solid line); q in units of π/d. The upper and lower bands correspond to Eqs. (7) and (8), respectively.

Further, using the Hilbert identity for Green's function of the 3D Helmholtz equation, we obtain the normalized wave functions (1):

$$\psi_{\kappa,q}(\mathbf{r}) = \frac{A(\kappa, q)}{\sqrt{L}} \left(\sum_{n=-\infty}^{\infty} \frac{\exp(-\kappa|\mathbf{r} - nd\mathbf{e}_z| + iqnd)}{|\mathbf{r} - nd\mathbf{e}_z|} - \frac{Q_1}{Q_2} \sum_{n=-\infty}^{\infty} \frac{\exp(-\kappa|\mathbf{r} - (nd + a)\mathbf{e}_z| + iqnd)}{|\mathbf{r} - (nd + a)\mathbf{e}_z|} \right), \tag{9}$$

where L is the crystal length and $A(\kappa, q)$ is the normalization factor:

$$A(\kappa, q) = \frac{1}{2} \left(\frac{\kappa d}{\pi} \frac{\cosh \kappa d - \cos qd}{\sinh \kappa d - \Re y} \right)^{1/2},$$

and

$$y = \frac{Q_1}{Q_2} (\exp[-iqd] \sinh \kappa a + \sinh \kappa [d - a]).$$

III. EXCITON SPECTRUM AND EIGENFUNCTIONS. BARE AND SCREENED e-h INTERACTION

Using the same arguments as in the 3D case one can show (see, for example, Ref. 10), that the wave equation for the Fourier transform ϕ of envelope function in the wave packet from products of the electron and hole Bloch functions, which represents a two-particle state of large-radius exciton at rest in a (quasi)one-dimensional semiconductor with period d, is reduced to the following 1D Schrödinger equation:

$$-\frac{\hbar^2}{2\mu} \phi''(z) + V(z)\phi(z) = \mathcal{E}\phi(z), \quad \mathcal{E} = E_{\text{exc}} - E_g, \quad -\infty < z < \infty, \tag{10}$$

where μ is the e-h reduced effective mass and $V(z)$ is the e-h interaction potential:

$$V(z) = -\int_{E_3^d}\int_{E_3^d} \times \frac{e^2}{((x_1-x_2)^2+(y_1-y_2)^2+(z+z_1-z_2)^2)^{1/2}} \times |u_{c;\kappa,\pi/d}(\mathbf{r}_1)|^2 |u_{v;\kappa,\pi/d}(\mathbf{r}_2)|^2 d\mathbf{r}_1 d\mathbf{r}_2, \times E_3^d = E_2 \times (0<z<d).$$

Here $u_{c,v;\kappa,q}(\mathbf{r})$ are the Bloch amplitudes of the Bloch wave functions $\psi_{c,v;\kappa,q}(\mathbf{r})=\exp(iqz)u_{c,v;\kappa,q}(\mathbf{r})$ of the conduction and valence band electrons of the linear crystal, respectively. Using the actual localization of the Bloch amplitudes at the crystal axis, after several Fourier transformations and simplifications we reduce the e-h interaction potential to the following form:

$$V_{r_1,r_2}(z) = -\frac{4e^2r_1^2}{r_2 d^2}\int_0^\infty \frac{J_1(k)J_1(kr_2/r_1)}{\kappa^4} \times \left(\frac{k}{r_1}(|d-z|+|d+z|-2|z|)+\exp\left[-\frac{k}{r_1}|d-z|\right] + \exp\left[-\frac{k}{r_1}|d+z|\right]-2\exp\left[-\frac{k}{r_1}|z|\right]\right)dk, \quad (11)$$

where J is the Bessel function of the first kind and r_1 and r_2 are the radii of transverse localization of the electron and hole wave functions, respectively:

$$r_{1,2} = \left(2\int_{E_2} r_{2D}^2 \int_0^L |u_{c,v;\kappa,q}(z,\mathbf{r}_{2D})|^2 dz d\mathbf{r}_{2D}\right)^{1/2},$$

where $\mathbf{r}_{2D}$ is the transverse component of the radius vector, $q=\pi/d$ and $\kappa=\kappa_{1,2}(\pi/d)$ correspond to the conduction and valence bands edges at the energy gap (according to Eqs. (7) and (8), respectively). Equation (10) with the potential given by (11) defines the spectrum of large-radius excitons in the linear, diatomic crystal if the effects of screening by the crystal electrons are ignored. Actually, the screening of the potential (11) by the band electrons is insignificant.

Indeed, following the Lindhard method (so-called RPA) to obtain the e-h interaction potential $\varphi(\mathbf{r})$ screened by the electrons of linear lattice, we consider the Poisson equation:

$$-\Delta\varphi(\mathbf{r}) = 4\pi(\rho^{\text{ext}}(\mathbf{r})+\rho^{\text{ind}}(\mathbf{r})) \quad (12)$$

where $\mathbf{r}$ is the radius vector, $\rho^{\text{ext}}(\mathbf{r})$ is the density of extraneous charge, and $\rho^{\text{ind}}(\mathbf{r})$ is the charge density induced by the extraneous charge (Δ is the Laplacian operator).

According to Eq. (12), the screened e-h interaction potential may be written as:

$$\varphi(\mathbf{r}) = 4\pi\int_{E_3}(\rho^{\text{ext}}(\mathbf{r}')+\rho^{\text{ind}}(\mathbf{r}'))G(\mathbf{r},\mathbf{r}')d\mathbf{r}', \quad (13)$$

where $G(\mathbf{r},\mathbf{r}')=1/(4\pi|\mathbf{r}-\mathbf{r}'|)$ is the Green's function of the 3D Poisson equation.

Let $E^0(q)$ and $\psi^0_{\kappa,q}(\mathbf{r})=\exp(iqz)u^0_{\kappa,q}(\mathbf{r})$ be the band energies and corresponding Bloch wave functions of the crystal electrons, and let $E(q)$ and $\psi_{\kappa,q}(\mathbf{r})$ be those in the presence of the extraneous charge. Then

$$\rho^{\text{ind}}(\mathbf{r}) = -e\sum_q [f(E(q))|\psi_{\kappa,q}(\mathbf{r})|^2 - f(E^2(q))|\psi^0_{\kappa,q}(\mathbf{r})|^2], \quad (14)$$

where f is the Fermi–Dirac function. Using the transverse localization of the Bloch wave functions near the crystal axis, in the approximation linear in φ we get:

$$\rho^{\text{ind}}(z',\mathbf{r}'_{2D}) = -e^2\sum_{q,q'}\frac{1}{E_{g;q,q'}}\int_0^L\int_{E_2} u_{v;\kappa_2,q'}(z,\mathbf{r}_{2D})u^*_{c;\kappa_1,q}(z,\mathbf{r}'_{2D})d\mathbf{r}_{2D}\varphi(z) \times \exp[iz(q'-q)]dz u^*_{v;\kappa_2,q'}(z',\mathbf{r}'_{2D})u_{c;\kappa_1,q}(z',\mathbf{r}'_{2D})\exp[iz'(q-q')], \quad (15)$$

where $E_{g;q,q'}=E_c(q)-E_v(q')$. Here and below, $\varphi(z)$ is the e-h interaction potential averaged in E_2 over the region of transverse localization of the Bloch wave functions and over the lattice period d along the crystal axis.

Due to the periodicity of the Bloch amplitudes ρ^{ind} may be written as:

$$\rho^{\text{ind}}(\mathbf{r}') = -\frac{e^2N}{L}\sum_{q,q'}\frac{C(q,q';d)}{E_{g;q,q'}}\varphi(q-q')u^*_{v;\kappa_2,q'}(\mathbf{r}')u_{c;\kappa_1,q}(\mathbf{r}') \times \exp[iz'(q-q')], \quad (16)$$

where

$$C(q,q';d) = \int_0^d\int_{E_2} u^*_{c;\kappa_1,q}(z,\mathbf{r}_{2D})u_{v;\kappa_2,q'}(z,\mathbf{r}_{2D})d\mathbf{r}_{2D}dz$$

and N is the number of unit cells in the crystal.

Further, after several transformations we obtain from (13) and (16) the one-dimensional Fourier transform of the potential φ:

$$\varphi(k) = \frac{\varphi_0(k)}{\varepsilon(k)},$$

TABLE I. Band gaps E_g and reduced effective masses μ according to Eqs. (7) and (8), radii of transverse localization r_1 and r_2 for electrons and holes, respectively, screening parameter g_d according to Eq. (22), and exciton binding energies $\mathcal{E}$ of the even and odd series for a linear diatomic crystal according to Eq. (10) with potential (11) for different values of the ratio $j=d/a$.

j	E_g, eV	μ (m_e)	r_1, nm	r_2, nm	g_d (10^{-6})	$\mathcal{E}_{0;\text{even}}$, eV	$\mathcal{E}_{1;\text{odd}}$, eV	$\mathcal{E}_{0;\text{even}}/E_g$
2.1	1.4422	0.041	0.070	0.0611	0.7235	–6.90	–0.5939	4.7845
2.3	3.3146	0.125	0.080	0.0569	2.4716	–8.9992	–2.0631	2.715
2.5	4.403	0.2199	0.088	0.0549	2.7036	–9.5352	–3.4812	2.1656
3	5.6281	0.5665	0.0994	0.0551	1.1206	–9.6588	–5.8421	1.7162

$$\varepsilon(k)=1+\frac{e^2N^2}{2\pi^2}\int_{-\pi/2}^{\pi/d}\frac{|C(q,q-k;d)|^2}{E_{g;q,q-k}}dq\widetilde{K}_0(k)\frac{2\sin(kd/2)}{kd} \tag{17}$$

where φ_0 is the Fourier transform of the averaged electrostatic potential induced by ρ^{ext}, and $\widetilde{K}_0(k)$ is the modified Bessel function of the second kind averaged over $\mathbf{r}_{2D}$ and $\mathbf{r}'_{2D}$ in the region of the transverse localization of Bloch wave functions in E_2, namely

$$\widetilde{K}_0(k)=\frac{1}{(\pi r_1 r_2)^2}\int_{E_2^{r_1}}\int_{E_2^{r_2}}K_0(|k||\mathbf{r}_{2D}-\mathbf{r}'_{2D}|)d\mathbf{r}_{2D}d\mathbf{r}'_{2D},$$

$$E_2^{r_i}=(0\leqslant r_{2D}\leqslant r_i)\times(0\leqslant\beta\leqslant 2\pi).$$

In the long-wavelength limit we get:

$$|C(q,q-k;d)|^2_{k\to 0}\approx|U(q;d)|^2k^2,$$

$$U(q;d)=\int_0^d\int_{E_2}u^*_{c;\kappa_1,q}(z,\mathbf{r}_{2D})\frac{\partial}{\partial q}u_{v;\kappa_2,q}(z,\mathbf{r}_{2D})d\mathbf{r}_{2D}dz. \tag{18}$$

Use of the Schrödinger equation for the orthogonal Bloch wave functions $\psi\kappa,q(\mathbf{r})$ yields

$$U(q;d)=\frac{i\hbar^2}{E_{g;q,q}m_b}\times\int_0^d\int_{E_2}\psi^*_{c;\kappa_1,q}(z,\mathbf{r}_{2D})\frac{\partial}{\partial z}\psi_{v;\kappa_2,q}(z,\mathbf{r}_{2D})d\mathbf{r}_{2D}dz. \tag{19}$$

Hence, in the long-wavelength limit the screened quasi-one-dimensional electrostatic potential induced by a charge e_0, distributed with the density

$$\rho^{\text{ext}}(z,\mathbf{r}_{2D})=\frac{e_0}{\pi R^2 d}(\Theta[z+d/2]-\Theta[z-d/2])\times(\Theta[r_{2D}]-\Theta[r_{2D}-R]),\quad R>0,$$

$$\Theta[x-x_0]=\begin{cases}0, & x<x_0,\\ 1, & x>x_0,\end{cases}$$

in accordance with (17) and (19), is given by the expression

$$\varphi(z)=\frac{8e_0r_1}{\pi d^2}\int_0^\infty\frac{(1/k^2)\sin^2(kd/2r_1)\widetilde{K}_0(k/r_1)\cos(kz/r_1)}{1+g_d(kr_1/d)\sin(kd/2r_1)\widetilde{K}_0(k/r_1)}dk \tag{20}$$

with

$$g_d=\left(\frac{e\hbar^2}{\pi r_1 m_b}\right)^2\int_{-\pi/d}^{\pi/d}\frac{1}{E^3_{g;q,q}}\left|\left\langle\psi_{c;\kappa_1,q}\left|\frac{\partial}{\partial z}\right|\psi_{v;\kappa_2,q}\right\rangle\right|^2dq. \tag{21}$$

According to equation (9) the dimensionless screening parameter g_d may be also written as:

$$g_d=\left(\frac{16e}{\hbar dr_1}\right)^2m_b\int_0^{\pi/d}\frac{A_c^2(\kappa_1,q)A_v^2(\kappa_2,q)}{(\kappa_2^2(q)-\kappa_1^2(q))^5}\times\left|\left(1+\frac{Q_1(\kappa_1,q)Q_1(\kappa_2,q)}{Q_2^*(\kappa_1,q)Q_2(\kappa_2,q)}\right)\int_{\kappa_1}^{\kappa_2}Q_1(\kappa,q)\,d\kappa-\frac{Q_1(\kappa_1,q)}{Q_2^*(\kappa_1,q)}\times\int_{\kappa_1}^{\kappa_2}Q_2^*(\kappa,q)\,d\kappa-\frac{Q_1(\kappa_2,q)}{Q_2(\kappa_2,q)}\int_{\kappa_1}^{\kappa_2}Q_2(\kappa,q)\,d\kappa\right|^2dq. \tag{22}$$

Note that κ_1 and κ_2 are the implicit functions of q defined by Eqs. (7) and (8), respectively.

It turns out that the values of g_d calculated according to (22) for d varying in the interval $[2.1a,3a]$ are about 10^{-6}.

IV. DISCUSSION. STABILIZATION OF SINGLE-ELECTRON STATES

Using Eqs. (7) and (8), we have obtained the band structure (see Fig. 1) and the electron and hole effective masses in a linear crystal of dimers for different values of the ratio $j=d/a$ of its period d to the distance a between atoms in the dimers. Besides, using wave equation (10) and potentials (11) and (20), we have found the large-radius exciton energy spectrum in the crystal for the bare e-h interaction and the e-h interaction screened by the bound electrons of the crystal. We present here results for a crystal with $j\in[2.1,3]$. Contrary to the single-band metallic crystal with $j=2$, the crystals with $j>2$ are semiconductors with band gaps varying from zero to the difference between the electron levels in an isolated dimer. In particular, the crystals with $j=2.001$ and realistic values of a and α (as in nanotubes and some 1D polymer chains) are narrow-gap semiconductors, in which

excitons may possess binding energies ~10 meV, but the crystals with $j=2.1$ are already wide-gap (~1 eV) semiconductors with strongly bound e-h pairs, and the crystals with $j=3$ are almost flat-band semiconductors, but their electrons and holes at the energy gaps ($q=\pi/d$) still have finite effective masses (these electrons and holes form the excitons in the crystals). For specificity, we have chosen the distance a equal to the graphite in-plane parameter 0.142 nm. The ZRP interaction parameter $\alpha=11.01$ nm^{-1} corresponds to the ionization energy of an isolated carbon atom ($E_{\text{ion}}=11.255$ eV).

As one can see from Table I, the dimensionless screening parameter obtained from (22) has values $g_d \ll 1$ for all the values of j considered. Thus it turns out that the screening of the e-h interaction potential by the band electrons in the linear diatomic crystal may be ignored. This result could be expected, since the linear crystal model under consideration is close to that of an electron gas confined to a cylindrical well. In the latter case, for which separation of the angular variables takes place, the states with different angular momentum quantum numbers m play the role of electron bands. Accordingly, the matrix element $|\langle\psi_c|\partial/\partial z|\psi_v\rangle|$ from (21) for the direct transitions between bands with different m turns out to be identically equal to zero. This is why only the binding energies of excitons with the unscreened interaction potential are listed in Table I.

To obtain estimates of the main characteristics of the linear crystal we considered several limiting cases. In the case of $d \gg a$ (or $j \gg 1$) and $a=$const, Eqs. (7) and (8) can be reduced to $\alpha - \kappa_{1,2} \mp \exp[-\kappa_{1,2}a]/a=0$, and thus the bands become flat ($\kappa_{1,2}$ do not depend on q) and the band gap tends to the finite value $(\hbar^2/2m_b)(\kappa_2^2-\kappa_1^2)$ (for $a=0.142$ nm it is about 6.3 eV); hence, the reduced effective mass and exciton binding energy tend to infinity, while the exciton radius $r_{\text{exc}} \sim \hbar^2/\mu e^2$ tends to zero. Therefore, the large-radius exciton theory is actually appropriate ($r_{\text{exc}} \ll a$) for excitons in a linear diatomic crystal only when its period d lies in the interval $(2a, 2.4a)$ (e.g., r_{exc} is $\sim 9a$ for $j=2.1$ and $\sim 2a$ for $j=2.4$). If $d=$const but $a \to 0$, the conduction band moves to the region of positive energies, and at some critical value of a it disappears, while the valence band shifts accordingly to the region of deep negative energies.

Table I shows that the ground-state exciton binding energies for linear diatomic crystals with any value of the ratio j are greater than the corresponding energy gaps. Note that according to the same calculations but with the bare mass $m_b=m_e$, the ground-state exciton binding energy for the linear crystal in vacuum turns out to be significantly greater than the energy gap. We should note also that the ground-state binding energies of excitons in linear crystals with different periods d in vacuum, calculated using the 1D analog of the Ohno potential[15] instead of potential (11), remain greater than the corresponding energy gaps. In particular, for $d=2.3a$ calculations with the 1D unscreened Ohno potential with the energy parameter U taken from Refs. 16 ($U=11.3$ eV) and 17 ($U=16$ eV) give the ground-state exciton binding energies $\mathcal{E}_{0;\text{even}}=5.90$ eV and $\mathcal{E}_{0;\text{even}}=7.63$ eV, respectively, while $E_g=3.31$ eV (see Table I). Thus, all calculations based on the solvable zero-range potentials model indicate the instability of the single-electron states in the vicinity of the energy gap with respect to the formation of excitons. This might be a shortcoming of this model, but it is worth mentioning that the results obtained within its framework for one-particle states in real 1D systems, like SWCNTs,[13,14] agree with existing experimental data in limits of accuracy of the latter.

The stability of single-electron states of 1D semiconductors with respect to exciton formation in vacuum can be explained by bringing multi-particle contributions into the picture. With the advent of some number of excitons in the quasi-one-dimensional crystal an additional screening appears, which is caused by the rather great polarizability of excitons in a longitudinal electric field. This collective contribution of born excitons to the crystal permittivity returns the lowest exciton binding energy $\mathcal{E}_{0;\text{even}}$ into the energy gap and so blocks further spontaneous transitions to the exciton states. To show this, let us consider the model of a linear crystal immersed in a gas of excitons with dielectric constant ε_{exc}, confined to the region of transverse localization of the carriers in the linear crystal, namely, a cylinder with radius r_1 and axis coinciding with that of linear crystal (from now on, for estimates, we assume that electron and hole have the same transverse localization radius). In this case it is easy to show that the e-h interaction potential is given by:

$$\varphi(z) = \frac{16e^2 r_1}{\pi d^2} \int_0^\infty \frac{\sin^2(kd/2r_1)\cos(kz/r_1)}{\varepsilon_{\text{exc}} k^4} \times \left(1 - \frac{2K_1(k)I_1(k)}{k(\varepsilon_{\text{exc}} K_0(k)I_1(k) + K_1(k)I_0(k))}\right) dk, \qquad (23)$$

where I_i and K_i are the modified Bessel functions of order i of the first and second kind, respectively. Further, as in Ref. 18, we use the known elementary relation between the permittivity of an exciton gas and its polarizability α in the direction of the linear crystal:

$$\varepsilon_{\text{exc}} = 1 + 4\pi\alpha, \quad \alpha = 2e^2 n \sum_k \frac{|\langle\Psi_0|\mathbf{r}|\Psi_k\rangle|^2}{\mathcal{E}_0 - \mathcal{E}_k},$$

where n is the bulk concentration of excitons, Ψ_0 and $\mathcal{E}_0$ are the exciton eigenfunction and binding energy which correspond to the ground state, and Ψ_k and $\mathcal{E}_k$ are those crresponding to all the excited states of the exciton. Thus the upper and lower limits for α are:

$$\frac{2e^2 n}{\mathcal{E}_0 - \mathcal{E}_1} |\langle\Psi_0|\mathbf{r}|\Psi_1\rangle|^2 \leqslant \alpha \leqslant \frac{2e^2 n}{\mathcal{E}_0 - \mathcal{E}_1} \sum_k |\langle\Psi_0|\mathbf{r}|\Psi_k\rangle|^2 = \frac{2e^2 n}{\mathcal{E}_0 - \mathcal{E}_1} |\langle\Psi_0|\mathbf{r}^2|\Psi_0\rangle|,$$

where Ψ_1 and $\mathcal{E}_1$ correspond to the lowest excited exciton state. Hence, one can obtain the upper and lower limits for n:

$$\frac{\varepsilon_{\text{exc}} - 1}{4\pi} \frac{\mathcal{E}_{0;\text{even}} - \mathcal{E}_{1;\text{odd}}}{2e^2} \left| \int_{-\infty}^{\infty} z^2 |\phi_0(z)|^2 dz \right|^{-1} \leqslant n,$$

$$n \leqslant \frac{\varepsilon_{\text{exc}} - 1}{4\pi} \frac{\mathcal{E}_{0;\text{even}} - \mathcal{E}_{1;\text{odd}}}{2e^2} \left| \int_{-\infty}^{\infty} z \phi_0(z) \phi_1(z) dz \right|^{-2}, \qquad (24)$$

where each ϕ is the component of Fourier transform of the corresponding exciton envelope function; it depends only on the distance z between the electron and hole. Here ϕ_0 is the

even solution of (10) with potential (23), which corresponds to the exciton ground state and satisfies the boundary condition $\phi'(0)=0$, and ϕ_1 is the odd solution of the same equation, which corresponds to the lowest excited exciton state and satisfies the boundary condition $\phi(0)=0$.

By varying ε_{exc} in (23) substituted into the wave equation (10) one can match $\mathcal{E}_{0;\text{even}}$ to the forbidden band width. Further, $\mathcal{E}_{1;\text{odd}}$ can be obtained from the same equation with the fixed ε_{exc} and with the corresponding boundary condition. All these magnitudes allow one to calculate from (24) rough upper and lower limits for the critical concentration of born excitons n_c sufficient to return $\mathcal{E}_{0;\text{even}}$ into the energy gap. Further, knowing n_c, we can calculate the shift of the forbidden band edges, which move apart due to the transformation of some single-electron states into excitons. This results in enhancement of the energy gap:

$$\delta E_g \simeq \frac{(\pi\hbar\tilde{n}_c)^2}{2\mu} \tag{25}$$

as in Ref. 19 and 20 Here $\tilde{n}_c=n_c\pi r_1^2$ is the linear critical concentration of excitons, and r_1 is the radius of electron wave functions transverse localization at the linear crystal axis.

In accordance with (24) the above-described model yields $\tilde{n}_c\sim 180\ \mu\text{m}^{-1}$ ($\sim 3\%$ of the number of atoms in the crystal) and $\sim 400\ \mu\text{m}^{-1}$ ($\sim 7\%$) for the linear crystal with $j=2.1$ and $j=2.3$, respectively, while according to Eq. (25) the corresponding δE_g are ~ 300 meV and ~ 500 meV in the same order. Here, however, we should mention that for SWCNTs both the measured[19,20] and similarly estimated[18] values of $\delta E_g/E_g$ turned out to be two to four times less.

Note, finally, that the instability of the single-electron states weakens or disappears for linear crystals immersed in dielectric media. As was shown in Ref. 9 for the example of the poly-para-phenylenevinylene 1D chain or in Refs. 16, 17, and 21 for the example of SWCNTs, the environmental effect may substantially decrease the exciton binding energies. Indeed, for the linear crystal in media even with permittivities $\varepsilon\sim$2-3 (e.g., like in Ref. 16 and 17) the ground-state exciton binding energy becomes smaller than the energy gap.

This work was supported by the Ministry of Education and Science of Ukraine, Grant #0106U001673.

[a)]Email: smyrnov@onu.edu.ua

[1]M. J. O'Connell, S. M. Bachilo, C. B. Huffman, V. C. Moore, M. S. Strano, E. H. Haroz, K. L. Rialon, P. J. Boul, W. H. Noon, C. Kittrell, J. Ma, R. H. Hauge, R. B. Weisman, and R. E. Smalley, Science **297**, 593 (2002).
[2]S. M. Bachilo, M. S. Strano, C. Kittrell, R. H. Hauge, R. E. Smalley, and R. B. Weisman, Science **298**, 2361 (2002).
[3]M. Ichida, S. Mizuno, Y. Saito, H. Kataura, Y. Achiba, and A. Nakamura, Phys. Rev. B **65**, 241407(R) (2002).
[4]F. Wang, G. Dukovic, L. E. Brus, and T. F. Heinz, Science **308**, 838 (2005).
[5]E. Chang, G. Bussi, A. Ruini, and E. Molinari, Phys. Rev. Lett. **92**, 196401 (2004).
[6]T. Ando, J. Phys. Soc. Jpn. **66**, 1066 (1997).
[7]A. Jorio, G. Dresselhaus, and M. S. Dresselhaus (eds.), *Carbon Nanotubes. Advanced Topics in the Synthesis, Structure, Properties and Applications*, Springer-Verlag, Berlin, Heidelberg (2008).
[8]S. Abe, J. Photopolym. Sci. Technol. **6**, 247 (1993).
[9]A. Ruini, M. J. Caldas, G. Bussi, and E. Molinari, Phys. Rev. Lett. **88**, 206403 (2002).
[10]V. M. Adamyan and O. A. Smyrnov, J. Phys. A: Math. Theor. **40**, 10519 (2007).
[11]S. Albeverio, F. Gesztesy, R. Høegh-Krohn, and H. Holden, *Solvable Models in Quantum Mechanics*, Texts and Monographs in Physics, Springer, New York (1988).
[12]Yu. N. Demkov and V. N. Ostrovskii, *Zero-Range Potentials and Their Applications in Atomic Physics*, Plenum, New York (1988).
[13]S. V. Tishchenko, Fiz. Nizk. Temp. **32**, 1256 (2006) [Low Temp. Phys. **32**, 953 (2006)].
[14]V. Adamyan and S. Tishchenko, J. Phys.: Condens. Matter **19**, 186206 (2007).
[15]K. Ohno, Theor. Chim. Acta **2**, 219 (1964).
[16]J. Jiang, R. Saito, Ge. G. Samsonidze, A. Jorio, S. G. Chou, G. Dresselhaus, and M. S. Dresselhaus, Phys. Rev. B **75**, 035407 (2007).
[17]R. B. Capaz, C. D. Spataru, S. Ismail-Beigi, and S. G. Louie, Phys. Rev. B **74**, 121401(R) (2006).
[18]V. M. Adamyan, O. A. Smyrnov, and S. V. Tishchenko, J. Phys.: Conf. Series **129**, 012012 (2008).
[19]Y. Ohno, S. Iwasaki, Y. Murakami, S. Kishimoto, S. Maruyama, and T. Mizutani, Phys. Rev. B **73**, 235427 (2006).
[20]O. Kiowski, S. Lebedkin, F. Hennrich, S. Malik, H. Rösner, K. Arnold, C. Sürgers, and M. M. Kappes, Phys. Rev. B **75**, 075421 (2007).
[21]V. Perebeinos, J. Tersoff, and P. Avouris, Phys. Rev. Lett. **92**, 257402 (2004).

This article was published in English in the original Russian journal. Reproduced here with stylistic changes by AIP.